

¹ **Submesoscale streamers exchange water on the north
2 wall of the Gulf Stream**

³ Jody M. Klymak¹, R. Kipp Shearman², Jonathan Gula³, Craig M. Lee⁴, Eric A. D'Asaro⁴, Leif N.
⁴ Thomas⁵, Ramsey Harcourt⁴, Andrey Shcherbina⁴, Miles A. Sundermeyer⁶, Jeroen Molemaker⁷
⁵ & James C. McWilliams⁷

⁶ ¹*University of Victoria, Victoria, British Columbia, Canada*

⁷ ²*Oregon State University, Corvallis, Oregon, USA*

⁸ ³*Laboratoire de Physique des Océans, Université de Bretagne Occidentale, Brest, France*

⁹ ⁴*Applied Physics Laboratory, University of Washington, Seattle, Washington USA*

¹⁰ ⁵*Stanford University, Stanford, California, USA*

¹¹ ⁶*University of Massachusetts Dartmouth, Dartmouth, Massachusetts, USA*

¹² ⁷*University of California, Los Angeles, California, USA*

¹³ **The Gulf Stream is a major conduit of warm surface water from the tropics to the subpolar
14 North Atlantic. Its north side has a strong temperature and salinity front that is maintained
15 for hundreds of kilometers despite considerable energy available for mixing. Large mesoscale
16 (> 20 km) “rings” often pinch off, but like the Gulf Stream they are resistant to lateral
17 mixing, and retain their properties for a long time. Here we observe and simulate a sub-
18 mesoscale (< 20 km) mechanism by which the Gulf Stream exchanges water with the cold
19 subpolar water to the north. The front exhibits a strong temperature-salinity contrast, with a
20 distinct mode of “mixed” water between the two water masses. This mass of water is not seen**

21 **to increase downstream despite there being substantial energy available for mixing. A series**
22 **of “streamers” detrain some of this water from the Gulf Stream at the crest of meanders.**
23 **Subpolar water is entrained replacing the mixed water, and helping to resharpen the front.**
24 **The water mass exchange can account for a northwards flux of salt of $0.8 - 5 \text{ psu m}^2\text{s}^{-1}$,**
25 **which can be cast as an effective local diffusivity of $O(100 \text{ m}^2\text{s}^{-1})$. This is similar to bulk-**
26 **scale flux estimates of $1.2 \text{ psu m}^2\text{s}^{-1}$ and is enough to supply fresh water to the Gulf Stream**
27 **as required for the production of 18-degree subtropical mode water.**

28 The Gulf Stream (GS) is the western boundary current of the North Atlantic subtropical
29 wind-driven circulation. It separates from Cape Hatteras and extends into the interior North At-
30 lantic, traveling east. As it does so, it loses heat not only to the atmosphere, but also by mixing
31 with the cold water in the subpolar gyre to the north. It also becomes fresher, an observation that
32 can only be explained by entrainment of fresh water from the north¹. As it entrains water, the GS
33 increases its eastward transport by approximately $4 - 8 \times 10^6 \text{ m}^3\text{s}^{-1}/100 \text{ km}$ (Johns et. al.²).

34 The GS has a sharp density front, but it also has a sharp temperature and salinity front, as has
35 been demonstrated at the surface from shipboard surveys³ and satellite images⁴. The sharpness of
36 the front beneath the surface has been less-clear, and requires high-resolution lateral sampling to
37 resolve. It is also known that the front has a sharp velocity gradient⁵, and such gradients act as a
38 barrier to lateral mixing^{6,7}. Despite this barrier, property budgets indicate that there is significant
39 exchange across the north wall¹, and that entrainment of fresh water is necessary to create the
40 dynamically important “18-degree water” that fills much of the upper Sargasso Sea.

41 The nature of this lateral mixing is opaque. There are large eddies that periodically pinch
42 off the GS and carry warm water to the north. However, some of these are re-entrained into the
43 GS and do not result in a net exchange. Instead, tracer budgets across the front appear to be
44 dominated by small-scale processes⁸. To date some of the best direct evidence for cross-front
45 exchange consists of the trajectories of density-following floats placed at the north wall^{9,10}. These
46 floats were observed to regularly detrain from the GS, such that of 95 floats, 26 stayed in the GS,
47 7 were detrained in rings, and 62 were detrained by mechanisms other than rings¹⁰. Kinematic
48 theories have been examined to explain the detrainment of the floats¹¹⁻¹³, and the similarity of the
49 float detrainment to satellite images of “streamers” of warm water detraining from the Gulf Stream
50 have been noted. However, direct observations of the processes as it occurs at depth have been
51 lacking.

52 Here we present evidence that there is small-scale mixing (<0.5 km) on the northern cy-
53 clonic side of the GS, and that the mixed water periodically peels off the GS in thin (5-10 km
54 wide) “streamers”. In March 2012 we made high-resolution measurements of the north wall of
55 the GS from 66 W to 60 W (Fig. 1), about 850 km east of where the GS separates from the North
56 American continental slope. Two research vessels tracked a water-following float placed in the GS
57 front and programmed to follow the density of the surface mixed layer. The float was transported
58 downstream with a speed of $1.4 \pm 0.2 \text{ m s}^{-1}$, in water that became denser as the surface of the GS
59 cooled. One vessel maintained tight sampling around the float and deployed an undulating profiler
60 to 200 m, making 10-km cross sections every 10 km downstream. The second vessel had an undu-
61 lating profiler making larger 30-km scale sections. Both profilers measured temperature, salinity

62 and pressure, and had approximately 1-km along-track resolution; both ships also measured ocean
63 currents. Fluorescent dye was deployed near the floats on some deployments, and measured by the
64 profilers on the ships. By following the float, a focus on the front was maintained as it curved and
65 meandered to the east.

66 During these observations, the GS had a shallow meander crest at 65 W (Fig. 1b) followed
67 by a long concave region (63 W) and then another large crest (61 W). Satellite measurements show
68 the sharp temperature changes across the front, superimposed with thin intermediate-temperature
69 ($15\text{-}18^{\circ}\text{C}$) streamers detraining to the north at approximately 65 W, 64 W, and at the crest of
70 the large meander at 61 W. An older streamer that has rolled up can also be seen at 62 W. The
71 ships passed through the three newer streamers providing the first detailed observations of their
72 underwater structure.

73 The front consists of density surfaces that slope up towards the north (Fig. 2a-d). The water
74 along density surfaces is saltier (and warmer) in the GS, and fresher (and colder) to the north.
75 The transition between the two water masses is remarkably abrupt, occurring over less than 5-km.
76 This sharpness persisted from our western-most section during the cruise (71.5 W) to the eastern-
77 most (60.5 W). Some cross sections clearly show lateral interleaving of salinity north of the front
78 (Fig. 2a) with approximately 5-km wide salinity anomalies ($S \approx 36.15 \text{ psu}$). These anomalies
79 move slower than the front (Fig. 2e), and have high potential vorticity that is normally associated
80 with the front (Fig. 2i).

81 The temperature-salinity (T/S) relationship of this data shows the contrast between the GS

82 and the subpolar water as two distinct modes (Fig. 3a), except near the surface where the water
83 masses are strongly affected by the atmosphere. For the deeper water, there is a third distinct popu-
84 lation between the two larger modes in T/S space that represents the water in the salinity anomalies,
85 and we have labelled as “streamers”. The distinctness of this water mass is remarkable, because
86 mixing processes usually are continuous, and we might have expected a more even distribution of
87 data between the two reservoirs. The distinctness in T/S space of the streamers indicates that after
88 the GS and subpolar waters mixed, the partially mixed water continued to mix, condensing it in
89 T/S space (perfectly mixed water would be a dot).

90 Looking at the GS in plan view (Fig. 3b) we see the mixed water that makes up the
91 streamers is connected along the length of our observations. The first streamer (64.5 W) is hor-
92 izontally connected over 100 km, and is about 5 km wide, and at least 150 m deep. Where the
93 streamer is the most detached (Fig. 2a) the main front is the sharpest of the 4 cross sections.
94 Downstream of this streamer, the mixed water thins before the eastern meander (60.5 W) where
95 there is a second streamer. Further downstream, the mixed water almost disappears by the last
96 cross-section (59 W). There is a hint of a streamer north of the front here, but our section did not
97 go far enough north to define it, but the thinning of the front is strong evidence that water has been
98 removed in a streamer.

99 We can quantify the rate of detrainment from the first streamer (64.5 W). It starts on the
100 fast side of the front with water flowing approximately 0.25 m s^{-1} faster than the float (Fig. 2h).
101 Upstream, where it is detached (Fig. 2e), it is flowing almost 0.5 m s^{-1} slower than the float. A

102 5-km wide and 150-m deep streamer, with a relative velocity of 0.75 m s^{-1} represents a rate of
103 detrainment of over $0.5 \times 10^6 \text{ m}^3 \text{ s}^{-1}$.

104 Concurrently, there is a bolus of fresh water from the north that is enfolded between the
105 streamers and the GS, which we will call an “intrusion”. The entrainment of the intrusion is hard
106 to quantify using the data presented above, because it is drawn from a large pool of water upstream.
107 However, a subsequent survey of the north wall (March 14) included a dye release in this water
108 that was then entrained in an intrusion (Fig. 4a-c). The streamer during this occupation was less
109 pronounced than the one described above, but was clear for a number of passes through the north
110 wall. The dye cloud was quite spread out, but the data show clear interleaving of the intrusion
111 water.

112 High-resolution numerical simulations ($dx \approx 500\text{m}$, see Methods) resolve these features
113 and also confirm the entrainment of the fresh intrusion (Fig. 4d-i). Seeding the simulation with La-
114 grangian particles (see methods) allows us to track the evolution of the streamers and the intrusion
115 as the flow moves downstream. Before the streamer is formed, the water in the intrusion (ma-
116 genta contours) is near the surface and the streamer water (green contours) is well within the front
117 (Fig. 4d,g). Downstream (Fig. 4e,h) the fresh water has been subducted to 150 m depth, and the
118 streamer has been pushed north of the front. Both water masses accelerate with the GS (Fig. 4f),
119 but the fresh intrusion accelerates more, such that the intrusion is entrained and the streamer slows
120 and is detrained. As in the observations, the streamer occupies an intermediate region in T-S space
121 (Fig. 4i, green contour), and originates in the high-vorticity region of the front. The acceleration

122 of the fresh intrusion relative to the streamer is an important finding of the model, as the fresh
123 water now forms a new sharp T-S front with the warm salty GS, and the mixed streamer water is
124 carried away from the front. The model further shows that the streamers are more prominent on
125 the leading edges of meanders, also clearly seen in satellite images (Fig. 1).

126 There are two major implications of the loss of mixed water to the north. The first is that
127 it helps explain why the front at the north wall of the GS remains so sharp. The T/S distribution
128 clearly indicate that there is mixing, and indeed the separate mode of water indicates that the
129 mixing is very vigorous. However we also show that the mixing product is carried away in the
130 streamers. It is striking that it is only the mixed water that is carried away, and not high-salinity
131 GS water (Fig. 3b) and that this is also high-vorticity water. This implies a dynamical link that
132 we have not seen explored. Streamers have been observed in surface temperature satellite images
133 and indirectly by subsurface floats^{9,11,14,15}, and this has led to kinematic models in which particles
134 are displaced from streamlines going around propagating meanders^{13,14,16}. The observations here
135 add to these models by showing that it is only mixed water that leaves the GS. This co-incidence
136 indicates to us a role for small-scale mixing in producing the destabilizing forces that cause this
137 water to detrain from the north wall. The observations and simulation indicate that the meanders
138 of the GS play an important role in the formation of the streamers.

139 The second implication is that the streamers are a mechanism that can balance large-scale
140 budgets that require significant exchange across the GS^{1,8}. Such budgets suggest that this region
141 of the GS loses salinity to the north at a rate of $1.2 \text{ psu m}^2 \text{s}^{-1}$ ¹. Each streamer transports 0.2 –

¹⁴² $0.5 \times 10^6 \text{ m}^3\text{s}^{-1}$ of water that is $0.8 - 1$ psu saltier than the water that is entrained. Streamers
¹⁴³ appear approximately every 100-300 km, associated with meanders, so an estimate of their average
¹⁴⁴ transport is $0.8 - 5$ psu m^2s^{-1} , bracketing the large-scale estimates. Working against a gradient
¹⁴⁵ of 1 psu/10 km over 200 m depth, the equivalent lateral diffusivity is $40 - 250 \text{ m}^2\text{s}^{-1}$. More
¹⁴⁶ observations would need to be made to make this transport estimate more robust.

¹⁴⁷ Here we have observed a submesoscale lateral stirring process along the north wall of the
¹⁴⁸ GS. The T/S front remains persistently sharp, despite small-scale mixing evident from the T/S dia-
¹⁴⁹ grams, and due to a number of possible processes^{17,18}. The mixed water mass does not accumulate,
¹⁵⁰ or it would weaken the sharpness of the front. Here we show that the streamers detrain the mixed
¹⁵¹ water, and entrain cold and fresh water toward the north wall, resharpening the temperature-salinity
¹⁵² front. Further analysis of the data and models will shed light on the exact mechanism triggering
¹⁵³ the ejection of water from the front via the streamers.

¹⁵⁴ **1 Methods**

¹⁵⁵ The Lagrangian float was placed in the Gulf Stream front based on a brief cross-stream survey,
¹⁵⁶ and programmed to match the density of the surface mixed layer (upper 30 m). The float moved
¹⁵⁷ downstream at a mean speed of 1.4 m s^{-1} . The *R/V Knorr* tracked the float and deployed a Chelsea
¹⁵⁸ Instruments TriAxis that collected temperature, salinity, and pressure (CTD) on a 200-m deep
¹⁵⁹ sawtooth with approximately 1-km lateral spacing in a 10-km box-shaped pattern relative to the
¹⁶⁰ float (Fig. 1, magenta). *R/V Atlantis* maintained a larger set of cross sections approximately 30 km

161 across the front, trying to intercept the float on each front crossing. *R/V Atlantis* was deploying a
162 Rolls Royce Marine Moving Vessel Profiler equipped with a CTD that profiled to 200 m approx-
163 imately every 1 km. Both ships had a 300 kHz RDI Acoustic Doppler Current Profiler (ADCP)
164 collecting currents on 2-m vertical scale averaged every 5 minutes (approximately 1 km lateral
165 scale), collected and processed using UHDAS and CODAS (<http://currents.soest.hawaii.edu>¹⁹).
166 This data reached about 130 m, and was supplemented at deeper depths with data from 75 kHz
167 RDI ADCPs, with 8-m vertical resolution.

168 Data were interpolated onto depth surfaces by creating a two-dimensional interpolation onto
169 a grid via Delauney triangulation. No extrapolation was performed. Data on the 26.25 kg m^{-3}
170 isopycnal were assembled at each grid point by finding the first occurrence of that isopycnal in
171 depth.

172 Potential vorticity is calculated from the three-dimensional grid as

$$q = -\frac{g}{\rho_0} (\nabla \times \mathbf{u} + \mathbf{f}) \cdot \nabla \rho, \quad (1)$$

173 where f is the Coriolis frequency, g the gravitational acceleration. The bracketed term is twice
174 the angular velocity, including the planet's rotation, and the gradient of density represents the
175 stretching or compression of the water column. In the GS, the potential vorticity is dominated by
176 contributions from the vertical density gradient and the cross-stream gradient of the along-stream
177 velocity:

$$q \approx N^2 \left(-\frac{\partial u}{\partial y} + f \right). \quad (2)$$

178 Dye Release. At select times during the float evolutions, fluorescein dye releases (100 kg
179 per release) were conducted at depth as close as possible to the float. Dye was pumped down a
180 garden hose to a tow package deployed off the side of the ship, consisting of a CTD and a dye
181 diffuser. Prior to injection, the dye was mixed with alcohol and ambient sea water to bring it to
182 within 0.001 kg m^{-3} of the float's target density. Initial dimensions of the dye streak were ≈ 1
183 km along-stream, ≈ 100 m cross-stream (after wake adjustment), and ranging from 1 - 5 m in the
184 vertical. The TriAxis system on the *R/V Knorr* tracked the fluorescein from its CTD package.

185 Numerical simulation. The high-resolution realistic simulation of the GS is performed with
186 the Regional Oceanic Modeling System (ROMS²⁰). This simulation has a horizontal resolution of
187 500m and 50 vertical levels. The model domain spans 1,000 km by 800 km and covers a region
188 of the GS downstream from its separation from the U.S. continental slope. Boundary conditions
189 are supplied by a sequence of two lower-resolution simulations that span the entire GS region and
190 the Atlantic basin, respectively. The simulation is forced by daily winds and diurnally modulated
191 surface fluxes. The modelling approach is described in detail in Gula et. al²¹.

192 Virtual Lagrangian Particles. The neutrally buoyant Lagrangian (flow-following) particles
193 were seeded at time 285 and advected both backwards and forwards from this time by the model
194 velocity fields without additional dispersion from the model's mixing processes²². A 4th-order
195 Runge-Kutta method with a time step $dt = 1$ s is used to compute particle advection. Velocity and
196 tracer fields are interpolated at the positions of the particles using cubic spline interpolation in both
197 the horizontal and vertical directions. We use hourly outputs from the simulation to get sufficiently

- 198 frequent and temporally-smooth velocity sampling for accurate parcel advection.
- 200
1. Joyce, T. M., Thomas, L. N., Dewar, W. K. & Girton, J. B. Eighteen degree water formation
201 within the Gulf Stream during CLIMODE. *Deep Sea Res. II* (2013).
 2. Johns, W., Shay, T., Bane, J. & Watts, D. Gulf stream structure, transport, and recirculation
203 near 68 w. *J. Geophys. Res.* **100**, 817–817 (1995).
 - 204 3. Ford, W., Longard, J. & Banks, R. On the nature, occurrence and origin of cold low salinity
205 water along the edge of the Gulf Stream. *J. Mar. Res.* **11**, 281–293 (1952).
 - 206 4. Churchill, J. H., Cornillon, P. C. & Hamilton, P. Velocity and hydrographic structure of sub-
207 surface shelf water at the Gulf Stream’s edge. *J. Geophys. Res.* **94**, 10791–10800 (1989). URL
208 <http://dx.doi.org/10.1029/JC094iC08p10791>.
 - 209 5. Rajamony, J., Hebert, D. & Rossby, T. The cross-stream potential vorticity front and its role
210 in meander-induced exchange in the gulf stream. *J. Phys. Oceanogr.* **31**, 3551–3568 (2001).
 - 211 6. Marshall, J., Shuckburgh, E., Jones, H. & Hill, C. Estimates and implications of surface
212 eddy diffusivity in the Southern Ocean derived from tracer transport. *J. Phys. Oceanogr.* **36**,
213 1806–1821 (2006).
 - 214 7. Naveira Garabato, A. C., Ferrari, R. & Polzin, K. L. Eddy stirring in the southern ocean. *J.*
215 *Geophys. Res.* **116** (2011).
 - 216 8. Bower, A. S., Rossby, H. T. & Lillibridge, J. L. The Gulf Stream-barrier or blender? *J. Phys.*
217 *Oceanogr.* **15**, 24–32 (1985).

- 218 9. Bower, A. & Rossby, T. Evidence of cross-frontal exchange processes in the Gulf Stream
- 219 based on isopycnal rafos float data. *J. Phys. Oceanogr.* **19**, 1177–1190 (1989).
- 220 10. Bower, A. S. & Lozier, M. S. A closer look at particle exchange in the Gulf Stream. *J. Phys.*
- 221 *Oceanogr.* **24**, 1399–1418 (1994).
- 222 11. Flierl, G., Malanotte-Rizzoli, P. & Zabusky, N. Nonlinear waves and coherent vortex structures
- 223 in barotropic β -plane jets. *J. Phys. Oceanogr.* **17**, 1408–1438 (1987).
- 224 12. Stern, M. E. Lateral wave breaking and “shingle” formation in large-scale shear flow. *J. Phys.*
- 225 *Oceanogr.* **15**, 1274–1283 (1985).
- 226 13. Pratt, L. J., Susan Lozier, M. & Beliakova, N. Parcel trajectories in quasigeostrophic jets:
- 227 Neutral modes. *J. Phys. Oceanogr.* **25**, 1451–1466 (1995).
- 228 14. Lozier, M., Pratt, L., Rogerson, A. & Miller, P. Exchange geometry revealed by float trajecto-
- 229 ries in the Gulf Stream. *J. Phys. Oceanogr.* **27**, 2327–2341 (1997).
- 230 15. Song, T., Rossby, T. & Carter, E. Lagrangian studies of fluid exchange between the Gulf
- 231 Stream and surrounding waters. *J. Phys. Oceanogr.* **25**, 46–63 (1995).
- 232 16. Bower, A. S. A simple kinematic mechanism for mixing fluid parcels across a meandering jet.
- 233 *J. Phys. Oceanogr.* **21**, 173–180 (1991).
- 234 17. Thomas, L. N. & Shakespeare, C. A new mechanism for mode water formation involving
- 235 cabbeling and frontogenetic strain at thermohaline fronts. In press *J. Phys. Oceanogr.*

- 236 18. Whitt, D. B. & Thomas, L. N. Near-inertial waves in strongly baroclinic currents. *J. Phys.*
237 *Oceanogr.* **43**, 706–725 (2013).
- 238 19. Firing, E., Hummon, J. M. & Chereskin, T. K. Improving the quality and accessibility of
239 current profile measurements in the southern ocean. *Oceanography* (2012).
- 240 20. Shchepetkin, A. & McWilliams, J. The regional oceanic modeling system (ROMS): a split-
241 explicit, free-surface, topography-following-coordinate oceanic model. *Ocean Modell.* **9**, 347–
242 404 (2005).
- 243 21. Gula, J., Molemaker, M. J. & McWilliams, J. C. Gulf stream dynamics along the southeastern
244 us seaboard. *J. Phys. Oceanogr.* **45**, 690–715 (2015).
- 245 22. Gula, J., Molemaker, M. J. & McWilliams, J. C. Submesoscale cold filaments in the gulf
246 stream. *J. Phys. Oceanogr.* **44**, 2617–2643 (2014).

247 List of Figures

258	2 Cross sections of data collected across the Gulf Stream. Y is the cross-stream	
259	distance perpendicular to the path of the float, positive being northwards. The four	
260	columns correspond to the four sections labeled a-d in Fig. 1. Potential density is	
261	contoured in black and $\sigma_\theta = 26.25 \text{ kg m}^{-3}$ is magenta. Along a constant density	
262	surface salty water is warmer than fresher water, so the GS on the left is warm	
263	and salty. Section a) is the furthest upstream section (65W) and d) is the furthest	
264	downstream (63.75 W) (Fig. 3b). e)-h) downstream velocity calculated relative to	
265	the float's trajectory by removing the float's mean speed of $u_{float} = 1.4 \text{ m s}^{-1}$ for	
266	the observation period. Green contours are regions in temperature-salinity space	
267	labeled “streamers” in Fig. 3a. i)-l) Potential vorticity sections (see text); 19	
268	3 Streamer properties and distribution in space. a) Logarithmically scaled his-	
269	togram in temperature-salinity space (colours). The warm-salty GS water is very	
270	distinct from the water to the north, which is cold and fresh. The water near the	
271	surface is heavily modified by the atmosphere. Deeper, there is a class of water	
272	distinct from the GS water and the water to the north, that we label “streamers”.	
273	This water is contoured in green in Fig. 2e-l. b) Interpolation of salinity, velocity,	
274	and potential vorticity onto the $\sigma_\theta = 26.25 \text{ kg m}^{-3}$ isopycnal, plotted geographi-	
275	cally (with a small exaggeration of scale in the north-south direction, and the latter	
276	two fields offset slightly to the south-east). This used data from both ships. The	
277	ship track for the <i>Atlantis</i> is plotted in black, and the four cross-sections in Fig. 2	
278	are plotted in magenta. The streamer water is contoured in green. 20	

302 **Acknowledgements** Our thanks to the captains and crews of *R/V Knorr* and *R/V Atlantis*, The AVHRR
303 Oceans Pathfinder SST data were obtained from the Physical Oceanography Distributed Active Archive Cen-
304 ter (PO.DAAC) at the NASA Jet Propulsion Laboratory, Pasadena, CA. <http://podaac.jpl.nasa.gov>. Funding
305 was supplied by Office of Naval Research, Grants XXXXXX

306 **Competing Interests** The authors declare that they have no competing financial interests.

307 **Correspondence** Correspondence and requests for materials should be addressed to Jody M. Klymak. (email:
308 jklymak@uvic.ca).

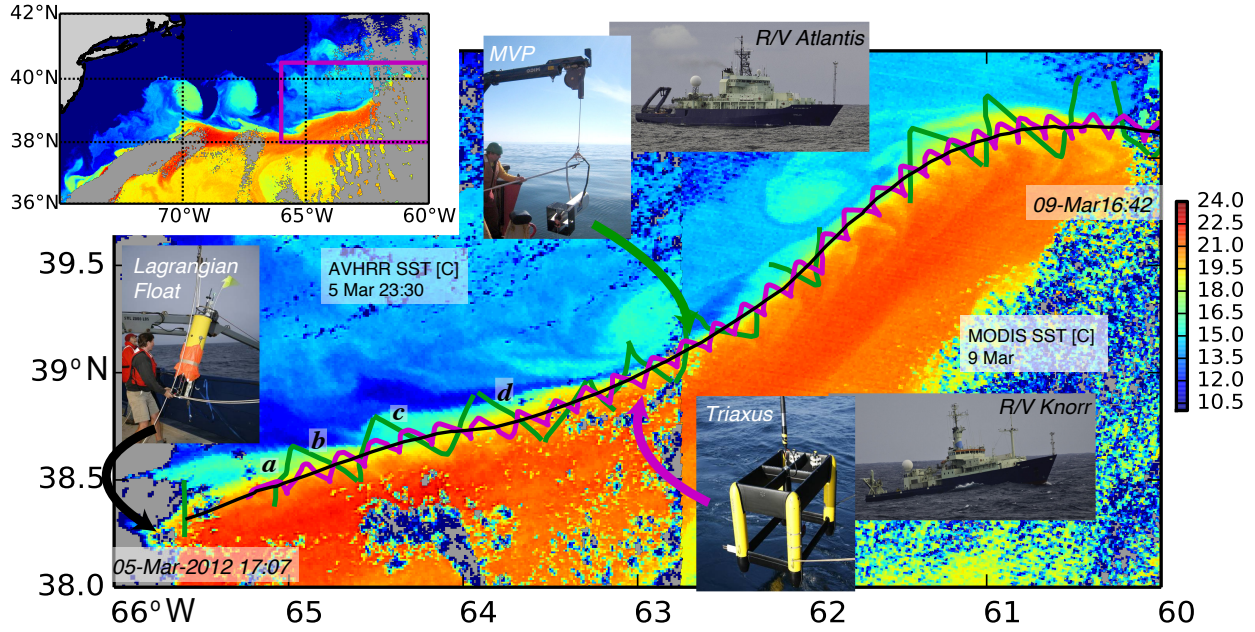


Figure 1: Experimental design. Inset: The experiment site on the north wall of the Gulf Stream, between 66 and 60 W, as shown in an AVHRR satellite image of sea surface temperature (SST). Main: Detailed SST image composed from two satellites images. The GS is warm and delineated by a sharp front. There are small sub-mesoscale structures north of the front, which are the focus of this paper. The satellite images are a composite from early in the observation period (AVHRR 6 Mar), and late (MODIS, 9 Mar). A Lagrangian float was deployed in the front (black curve), and the ship tracks bracketed the float's position (green: *R/V Atlantis*, magenta: *R/V Knorr*). *R/V Atlantis* cross-sections labeled a-d are shown in Fig. 2a-d.

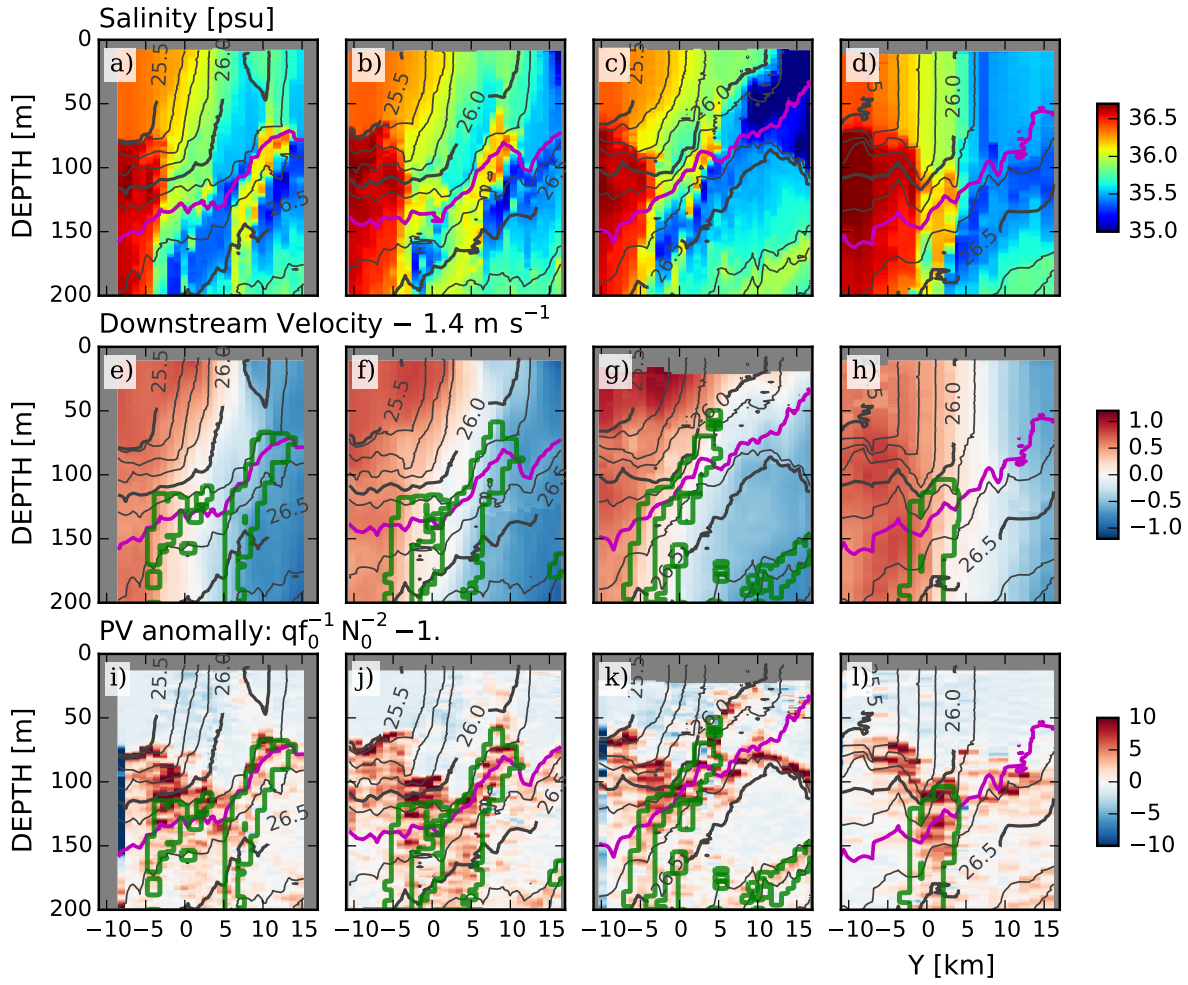


Figure 2: Cross sections of data collected across the Gulf Stream. Y is the cross-stream distance perpendicular to the path of the float, positive being northwards. The four columns correspond to the four sections labeled a-d in Fig. 1. Potential density is contoured in black and $\sigma_\theta = 26.25 \text{ kg m}^{-3}$ is magenta. Along a constant density surface salty water is warmer than fresher water, so the GS on the left is warm and salty. Section a) is the furthest upstream section (65W) and d) is the furthest downstream (63.75 W) (Fig. 3b). e)–h) downstream velocity calculated relative to the float's trajectory by removing the float's mean speed of $u_{\text{float}} = 1.4 \text{ m s}^{-1}$ for the observation period. Green contours are regions in temperature-salinity space labeled “streamers” in Fig. 3a. i)–l) Potential vorticity sections (see text);

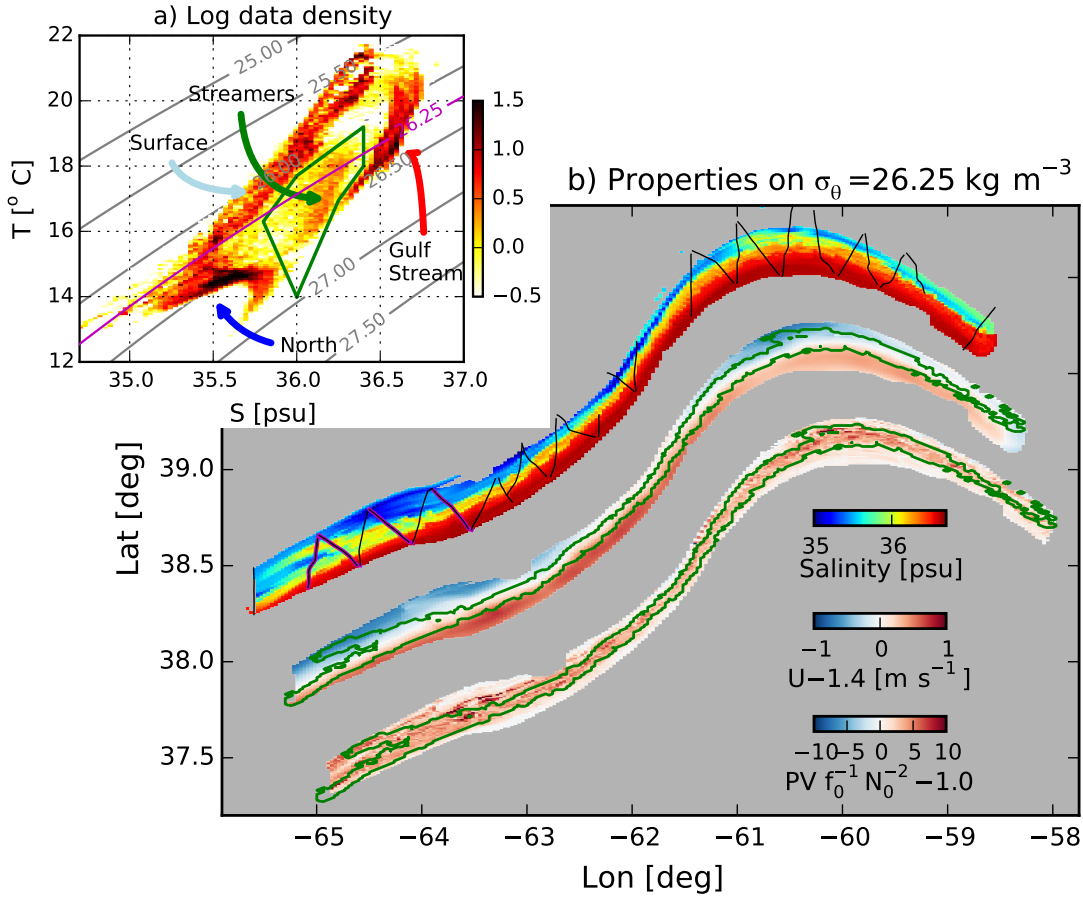


Figure 3: Streamer properties and distribution in space. a) Logarithmically scaled histogram in temperature-salinity space (colours). The warm-salty GS water is very distinct from the water to the north, which is cold and fresh. The water near the surface is heavily modified by the atmosphere. Deeper, there is a class of water distinct from the GS water and the water to the north, that we label “streamers”. This water is contoured in green in Fig. 2e-l. b) Interpolation of salinity, velocity, and potential vorticity onto the $\sigma_\theta = 26.25 \text{ kg m}^{-3}$ isopycnal, plotted geographically (with a small exaggeration of scale in the north-south direction, and the latter two fields offset slightly to the south-east). This used data from both ships. The ship track for the *Atlantis* is plotted in black, and the four cross-sections in Fig. 2 are plotted in magenta. The streamer water is contoured in green.

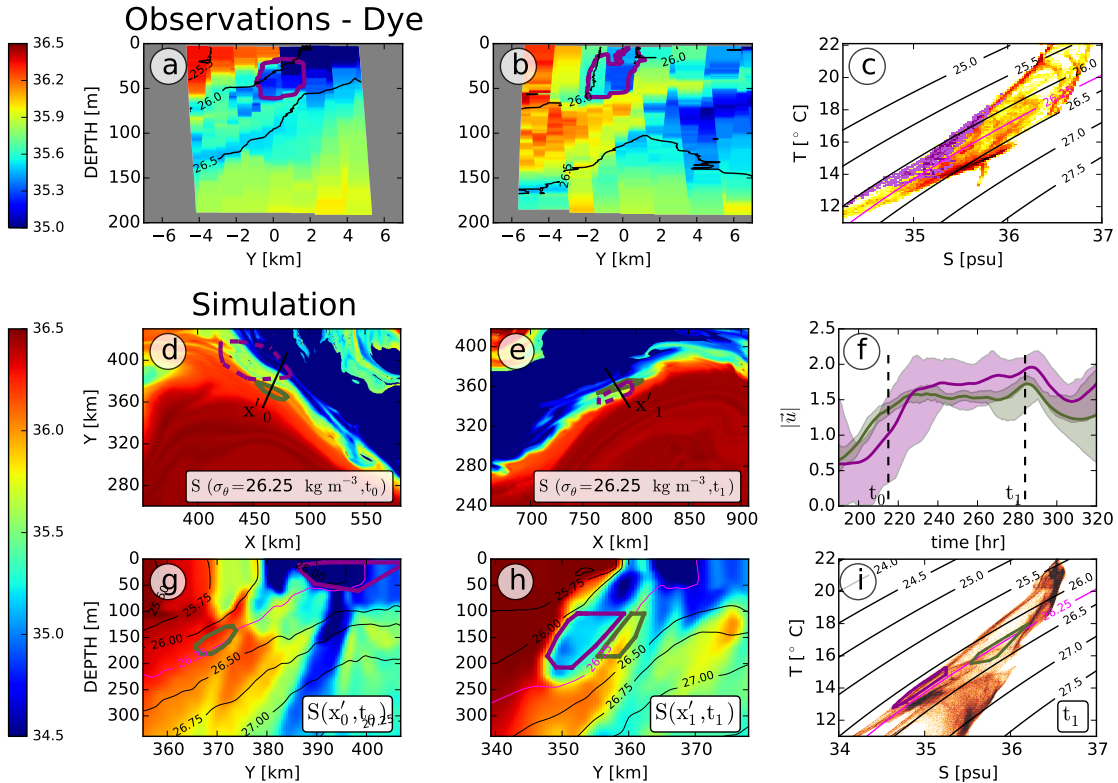


Figure 4: **Evidence for entrainment of intrusions from a dye release and numerical simulation.**

a) Salinity section from an occupation of the GS 14 March. The location of a dye is contoured in magenta. b) Salinity section from downstream. A streamer has enfolded the dye in cold-fresh water between itself and the GS. c) Temperature-salinity diagram for this occupation. The temperature-salinity for the dye is coloured in dark magenta. d) Salinity in the GS on the $\sigma_\theta = 26.25 \text{ kg m}^{-3}$ isopycnal from a high-resolution numerical simulation at t_0 . The green contours delineate the location of particles seeded downstream in the streamer at time $t_1 = t_0 + 70\text{h}$ (see panels e and h) and advected *backwards* in time to t_0 showing where the streamer water originated. The dark magenta contour is the location of particles seeded in the fresh intrusion. The straight line shows the location of the salinity cross-section in panel g. e) as panel d, except at $t_1 = t_0 + 70\text{ h}$; this is the time and locations where the two clouds of particles were seeded. g) and h) salinity cross sections for times t_0 and t_1 . The location of the particles is shown in green and dark magenta contours. The $\sigma_\theta = 26.25 \text{ kg m}^{-3}$ isopycnal is contoured in light magenta. These panels show that the origin of the streamer water was in the GS front, and that the fresh-cold water